Hindawi
Advances in Civil Engineering
Volume 2018, Article ID 4802075, 17 pages
https://doi.org/10.1155/2018/4802075

Research Article

Strata Movement and Fracture Propagation Characteristics due to Sequential Extraction of Multiseam Longwall Panels

Xiangyang Zhang,[1] **Behrooz Ghabraie**,[2] **Gang Ren**,[2] **and Min Tu**[1]

[1]*School of Mining and Safety Engineering, Anhui University of Science and Technology, Huainan, Anhui, China*
[2]*School of Engineering, RMIT University, Melbourne, Australia*

Correspondence should be addressed to Xiangyang Zhang; xyzhang@aust.edu.cn

Received 28 August 2018; Accepted 19 November 2018; Published 27 December 2018

Guest Editor: Zhanguo Ma

Multiseam longwall mining-induced strata deformation and fracture propagation patterns are different from those of single-seam mining. This difference is due to interaction of the caved zones as a result of longwall mining activity at different coal seams, which severely impacts formation of subsidence and permeability of the strata after multiseam mining. Understanding this phenomenon is of great importance in order to predict the multiseam subsidence reliably, evaluate the risk of water inrush and take suitable preventive measures, and determine suitable locations for placing gas drainage boreholes. In this study, scaled physical modelling techniques are utilised to investigate strata deformation, fracture propagation characteristics, and vertical subsidence above multiseam longwall panels. The results show that magnitude of the incremental multiseam subsidence increases significantly after multiseam extraction in comparison with single-seam mining. This increase occurs to different extent depending on the multiseam mining configuration. In addition, interstrata fractures above the abutment areas of the overlapping panels propagate further towards the ground surface in multiseam extractions compared with single-seam extractions. These fractures increase the risk of water inrush in presence of underground/surface water and create highly permeable areas suitable for placing gas drainage boreholes.

1. Introduction

Longwall mining is a caving method, in which the roof of the extracted longwall panels is left unsupported, allowing the immediate strata cave into the extracted zone [1]. As a result, overburden layers cave and deform, creating three different zones (Figure 1): (1) caved zone, (2) fractured zone, and (3) continuous deformation zone [2, 3]. Height of these zones can vary in accordance with site-specific parameters [2, 4, 5]. The fracture propagation pattern within the caved and fractured zones (Figure 1) results in increased hydraulic conductivity of the strata after longwall mining. Understanding the hydraulic conductivity of the overburden strata is of great significance, especially in case of longwall mining under water bodies [6, 7]. The induced fracture network in the caved zone can interact with underground water, providing the water with a flow path towards the workings and increasing the risk of water inrush [6]. In addition, increased hydraulic conductivity and permeability of the caved and fractured zones provides a potential inflow path for releasing methane gas from coalbeds into low-pressure caved and fractured areas [8]. Understanding this phenomenon is important in order to employ suitable methane gas drainage strategies [2]. Furthermore, in subsidence analysis, understanding the strata deformation pattern provides insights into the ground surface subsidence mechanism. This understanding helps in modifying subsidence prediction methods in order to achieve reliable subsidence predictions after longwall mining [9–12]. In recent years, by decreasing the number of untouched coal seams, multiseam longwall mining has become increasingly more popular [13]. However, field observations from various multiseam mine sites around the world and research works in the literature show that the induced strata and ground surface movement profiles after multiseam extraction vary from case to case and are different from those of single-seam

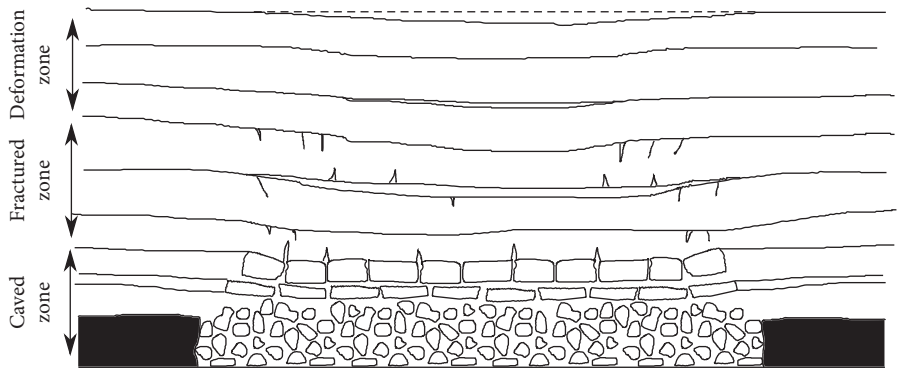

Figure 1: Different zones above an extracted longwall panel (adapted from [1]).

mining [14–18]. In fact, as mentioned in [19], multiseam subsidence is a case-dependent phenomenon which is influenced by variations in arrangement of the workings in coal seams, geology and thickness of the interburden, and mining methods. Ghabraie et al. [11, 12, 20] demonstrated via physical models that interaction of the old caved and disturbed areas as a result of the first mining activity with the newly induced caved and disturbed areas as a result of a newly extracted multiseam longwall panel generates changes in the strata deformation mechanism. Also, a case of caving and fracture propagation pattern physical and numerical modelling performed in [17] indicated that the height of the caved zone and, thus, height of the water conductive zone above multiseam longwall panels are significantly greater than those of the resultant caved and water conductive zones above single-seam panels. These observations together with available research studies in the literature (for example, [11, 21, 22, 23]) show that because of the interaction of the caved and fractured zones from multiple mining activities, strata deformation and fracture propagation patterns, and thus variations in the hydraulic conductivity of the strata, after multiseam mining are severely different from those of single-seam mining.

The aim of this study is to investigate the ground movement characteristics and fracture propagation pattern due to multiseam longwall coal mining by means of physical modelling techniques. Physical modelling techniques provide the opportunity to readily observe the actual fracture propagation pattern and strata movement characteristics after sequential extraction of longwall panels [23, 24]. This ability makes physical modelling techniques a suitable method for achieving the purpose of this study. Three case studies are modelled by means of physical modelling methods. The physical models have different panel arrangements, interburden thicknesses, and geology and sequences of extraction. Similarity theory principles are utilised to ensure reliability of measurements from physical models. The models are tested and compared with each other based on three main parameters: (1) strata deformation pattern, (2) fracture propagation pattern, and (3) vertical subsidence at different distances above each longwall panel. Based on the physical modelling results, strata movement and multiseam subsidence characteristics are explained in accordance with mining configuration and effects of previously caved and fractured zones. In addition, fracture propagation patterns from sequential extraction of multiseam panels and its effect on hydraulic conductivity of the strata are discussed. Based on the fracture propagation pattern after multiseam mining, risk of water inrush and suitable location for high productive gas drainage boreholes are also evaluated.

2. Case Studies

To study the effects of multiseam mining on strata deformation characteristics and fracture propagation pattern, two case studies and an extension of the second case study were modelled via physical modelling techniques (Figure 2). The two case studies are the Shuoli coal mine, located approximately 20 km northeast of the Huaibei city, Anhui Province, China (Figure 2(a)), and the Panyidong coal mine, located approximately 30 km northwest of Huainan city, Anhui Province, China (Figure 2(b)). Schematic arrangement of the panels in these two case studies is shown in Figure 2. The third case study was designed to investigate the effect of extending the upper panel to its left in the second case study, Panyidong coal mine (Figure 2(b)).

In the following sections, Shuoli and Panyidong mine case studies are referred to as Case 1 and Case 2, respectively, and extension of the upper panel in the Panyidong mine case study is referred to as Case 3.

2.1. Geology of the Case Studies

2.1.1. Case 1. There are two mining seams at the Shuoli mine: coal seam no. 3 (upper seam) and coal seam no. 5 (lower seam). The coal seams are mostly flat at a depth of approximately 305 m. The lower seam is located 12 m beneath the upper layer. Detailed lithology of the mine site is noted in Table 1. In this case study, the upper seam is mined first following extraction of the lower seam. Both seams are mined using the mechanised longwall mining method. Panel dimensions at the modelled section of this case study are noted in Table 2.

2.1.2. Case 2. The overburden thickness above coal seam no. 13-1 (upper seam) in the Panyidong mine is approximately 770 m. Approximately 66 m under the upper seam, coal

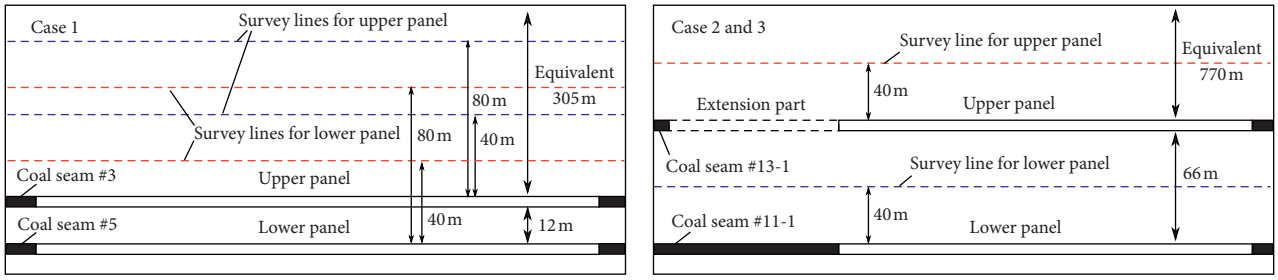

Figure 2: Schematic view of the panel arrangements and survey lines for subsidence measurements in (a) Case 1 and (b) Cases 2 and 3.

Table 1: Lithology of Case 1.

Rock mass	Depth (m)	Thickness (m)	Rock mass description
Mudstone and siltstone	296.37	296.37	Mudstone: dark grey, including carbon in section and iron-sandstone. Siltstone: grey, massive block, simple structure containing fossil plant pieces
Medium-grained sandstone	301.47	5.1	Medium-grained sandstone: grey, blocky, mineral composition with quartz
Mudstone	304.11	2.64	Mudstone: blocky, uniform, with fossil pieces
Coal seam no. 3	306.17	2.06	Coal: black, powdery, dim glossiness, unclear structure
Mudstone and medium-grained sandstone	318.17	12	Mudstone: blocky, simple structure with fossil plant pieces. Medium-grained sandstone: grey, massive block, mineral composition with strong quartz
Coal seam no. 5	321.39	3.22	Coal: black, blocky, bright coal, lightweight, and crisp
Sandy mudstone	324.41	3.02	Sandy mudstone: dark grey, blocky, simple structure with fossil pieces
Fine sandstone	331.59	7.18	Fine sandstone: light grey, blocky, uniform mineral composition

Table 2: Panel dimensions and extraction sequence of all the case studies.

Case study	Coal seam	Longwall panel	Extraction sequence	Panel width (m)	Average thickness (m)
Case 1	Coal seam #3	Upper panel	First	210	2
	Coal seam #5	Lower panel	Second	220	3.2
Case 2	Coal seam #13-1	Upper panel	Second	210	3
	Coal seam #11-1	Lower panel	First	210	2.45
Case 3	Coal seam #11-1	Extension part	—	100	3

seam no. 11-1 (lower seam) is located. Both coal seams are mostly flat and are extracted using the mechanised longwall mining method. Detailed lithology of this mine site is noted in Table 3. In this case study, the lower panel is extracted before extraction of the upper panel. This is due to high gas content of the upper seam and the fact that extraction of the lower panel before the upper panel would effectively decrease the methane gas pressure and reduce the risk of outburst. Panel dimensions at the modelled section of this case study are noted in Table 3.

2.1.3. Case 3. As mentioned above, Case 3 is an extension of Case 2. Lithology, sequence of extraction, and overburden thickness are the same as those in Case 2. In this case study, in the same physical model of Case 2, the upper panel is extended to 100 m with the same extraction thickness as that of the upper seam in Case 2. This extraction is referred to as the extension part (Table 3).

3. Physical Modelling Principles

3.1. Similarity Theory. Strata movement characteristics and crack propagation pattern can be effectively investigated by means of scaled physical modelling if built in accordance with laws of similarity theory [12, 25]. As Whittaker and Reddish mentioned in 1989, only parameters with major influence on the mechanical behaviour of the material need to be considered in calculating the similarity ratios, such as density and strength of the material and geometry of the model and every feature in the model. These parameters should follow the following relationship:

Table 3: Lithology of Case 2.

Rock mass	Depth (m)	Thickness (m)	Rock mass description
Mudstone and siltstone	756.13	760	Mudstone: dark grey, carboniferous iron-sandstone; siltstone: grey, blocky, simple structure with fossil pieces
Fine sandstone	767.66	11.53	Fine sandstone: light grey, fine-grained texture, mineral composition with hard quartz
Mudstone	769.6	1.94	Mudstone: dark grey, blocky, fragile carboniferous with fossil pieces
Coal seam no. 13-1	772.6	3	Coal: black, blocky dull coal, with bright coal and specular coal bands, belongs to semibright and semidull coal
Sandy mudstone and fine sandstone	838.7	66.1	Sandy mudstone: grey, sandy texture with muddy band, composition includes carbon in the part area, fragile. Fine sandstone: light grey, fine grained, mineral composition includes hard quartz and sandy mudstone
Coal seam no. 11-1	841.3	2.45	Coal: black, blocky dull coal, includes bright coal and specular coal bands, belongs to semibright coal
Sandy mudstone	848.2	2.6	Sandy mudstone: grey, sandy texture, fragile with fossil pieces
Sandy mudstone	855.1	6.9	Sandy mudstone: grey to dark grey, mainly sandy texture with little carbon and fine texture

$$\frac{C_\sigma}{C_p \times C_l} = 1, \tag{1}$$

where C_l, C_σ, and C_p are constants of geometry (length), strength, and density similarity, respectively. Equation (1) is referred to as the fundamental condition of the similarity theory [20, 25]. In this equation, C_l, C_σ, and C_p can be calculated as follows:

$$C_l = \frac{L_p}{L_m},$$
$$C_\sigma = \frac{\sigma_p}{\sigma_m}, \tag{2}$$
$$C_p = \frac{\rho_p}{\rho_m},$$

where L_p and L_m are the length of the prototype case and model, respectively; σ_p and σ_m are the strength (UCS) of the prototype case and model, respectively; and ρ_p and ρ_m are the density of the prototype case and model, respectively.

3.2. Model Construction. Longwall panels are commonly larger in one dimension (length) than the other (width). As a result, it can be assumed that the effects of start and end of a longwall panel are negligible on a middle section of the panel; that is, a section of a panel can be modelled in the plane stress condition.

The physical model for Cases 1 and 2 is 3 m long, 2.6 m high, and 0.3 m thick and 4 m long, 3 m high, and 0.4 m thick, respectively. Similarity theory constants considered for construction of the model and test materials are $C_l = 1:100$, $C_\rho = 1:1.67$, and $C_\sigma = 1:167$. Physical model materials are constructed by means of mixtures of sand, kalk, and plaster of various ratios. These ratios result in suitable strength and density values for the model material based on the mentioned similarity constants. Prototype material strength and density values are noted in Table 4. Material strength parameters for the physical models can be readily calculated using the abovementioned similarity theory constants and the values noted in Table 4. To be able to assist separation of the rock layers after extraction of the longwall panels, a thin layer of kalk is used in between each layer to simulate bedding surfaces.

Panel dimensions and extraction thickness for all the models are noted in Table 2. Only a section of the overburden layers is modelled in the physical models, and equivalent load of the rest of the overburden layers, based on the average depth of the panels (Figure 2), is applied on the model top part to simulate the weight of the overburden layers. In this regard, weight of 60 kN for Case 1 and 85 kN for Case 2 (and Case 3), by means of the loading method shown in Figure 3, is applied on the top part of the models.

Extraction of the longwall panels is simulated by sequential removal of the coal seams. The extraction rate in all cases is considered as 5 cm per 2 hours. This extraction rate represents extraction of 5 m of coal seam per day. In this way, adequate time is given for the strata to deform after extraction of each section of the coal seam.

3.3. Monitoring Method. The photogrammetry method, as explained in [20], is utilised to monitor strata movement characteristics and fracture propagation pattern in all case studies. For this purpose, digital photos after completion of various stages of the tests have been captured and compared. Resolution of the photographs limits the entries in Table 4. Model construction material strength properties can be readily calculated using similarity constants.

Table 4: Prototype material properties and mixture proportions of the construction material.

Rock mass	Prototype rock mass parameters				Model mixture
	Compressive strength (MPa)	Tensile strength (MPa)	Density (kg/m^3)	Poisson's ratio	Sand : kalk : plaster
Fine sandstone	98.76	1.03	2600	0.23	6 : 0.6 : 0.4
Mudstone	35.70	0.07	2680	0.25	7 : 0.7 : 0.3
Coal	18.87	0.03	1530	0.21	10 : 0.5 : 0.5
Siltstone	11.45	0.83	2591	0.22	9 : 0.5 : 0.5
Sandy mudstone	42.52	0.33	2720	0.22	8 : 0.7 : 0.3
Fine sandstone	90.42	1.06	2660	0.22	6 : 0.6 : 0.4
Medium-grained sandstone	60.45	0.55	2700	0.23	8 : 0.7 : 0.3

Figure 3: Loading devices used for physical models.

Given the resolution of the photographs in this study, strata deformation is measured to an accuracy of approximately +/−1 mm [20].

4. Physical Modelling Results

Figures 4 and 5 show the physical models at different stages of the tests in the three case studies. In the following sections, observed strata movement, fracture propagation patterns, and ground subsidence are reported in detail.

4.1. Strata Deformation Pattern. The major strata deformation pattern is investigated by considering 5% of the maximum deformation after each extraction as the limit of the strata deformation. This limit results in deformations more than the minimum accuracy of the monitoring method and at the same time illustrates the major deformation pattern of the strata. In the following sections, only the incremental strata deformations due to extraction of the multiseam panels are reported in order to investigate the effect of extraction sequence of the multiseam mining cases.

4.1.1. Case 1. By extraction of the lower panel, significant deformations are induced within the interburden area and the disturbed overburden strata, especially above the newly extracted segment (Figure 6(b)). Extracting this segment also creates some deformation above the to-be-extracted segments. It can be seen that, unlike single-seam extractions, the limit of the ground movement due to extraction of the first segment of the lower seam is located beyond its edge. This extended affected area, however, is located within the disturbed area resulting from the previously extracted upper panel (trapezoid grey-shaded area in Figure 6(a)).

Similarly, extraction of the second segment of the lower coal seam induces significant deformation directly above the newly extracted segment and above the previously extracted segment of the lower panel. A smaller magnitude of deformation is observed above the to-be-extracted segment in comparison with the area above the newly extracted segment (Figure 6(c)).

Extracting the third (last) segment of the lower seam enhances the ground movement on a larger area compared with the previous two segments (by comparison of the red-shaded area in Figure 6(d) with those in Figures 6(b) and 6(c)). In addition, significant deformations are induced in shallower layers (top part of the model) within the previously disturbed overburden strata. Extraction of the lower panel results in no significant displacement beyond the limit of the previously disturbed zone (grey-shaded area). In other words, the effect of multiseam mining in this case is mostly limited to the extent of the first mining activity above the edges of the extracted panels and topmost layer of the model.

4.1.2. Case 2. In Case 2, the lower panel is mined completely before extraction of the upper panel commences. The strata movement pattern for the lower seam is similar to that in Case 1 (Section 4.1.1) with a slightly wider limit of the major strata movement (Figure 7(a)), which is a result of a greater depth, and thus greater load on this panel in comparison with the upper panel extraction in Case 1 (Figure 6(a)).

Similar to Case 1, sequential extraction of the multiseam panel results in enhanced subsidence directly above the extracted segments and relatively smaller magnitude of deformation above the to-be-extracted segments, which are located within the previously disturbed area (grey-shaded area in Figures 7(b) and 7(c)). After extracting the last segment of the upper panel (Figure 7(d)), the resultant deformation remains within the previously disturbed area and indicates a rather sharp angle of major deformations at the edge of the upper panel in comparison with the single-seam mining (by comparison of deformation pattern at the left edge of the last segment in Figure 7(d) and that of the lower panel in Figure 7(a)).

4.1.3. Case 3. In Case 3, the asymmetric multiseam mining configuration is investigated by extending the upper panel to its left in the second case study (Section 4.1.2). Extracting the first segment of the extension part induces significant

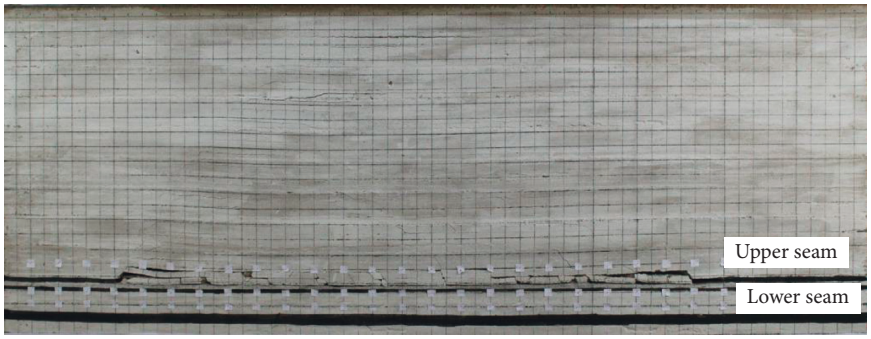

(a)

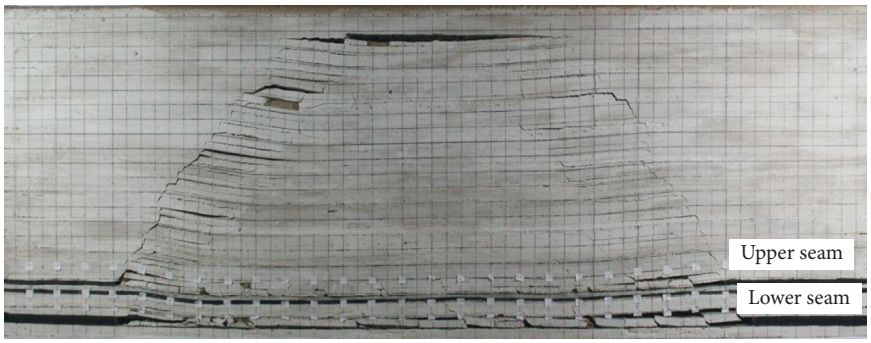

(b)

Figure 4: Physical modelling results after extraction of (a) upper and (b) lower panels in Case 1.

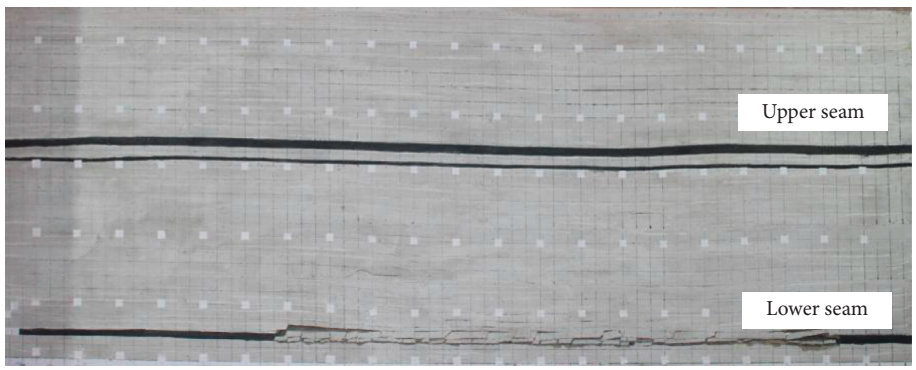

(a)

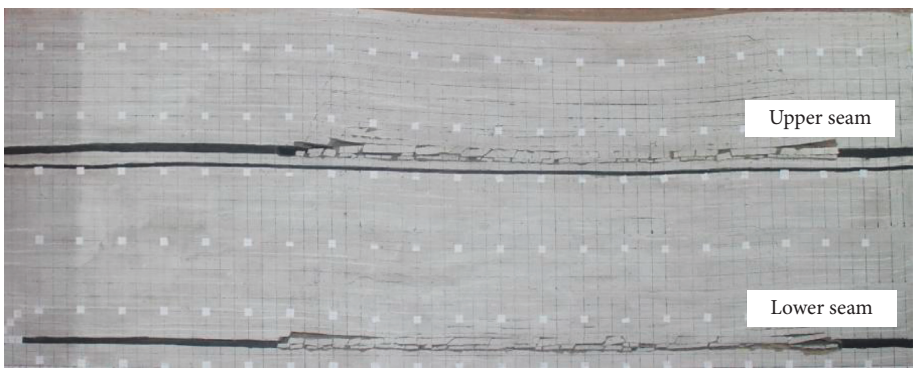

(b)

Figure 5: Continued.

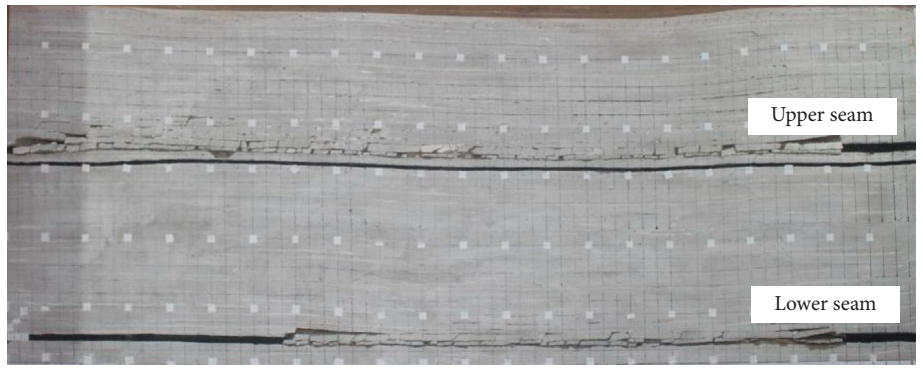

(c)

Figure 5: Physical modelling results after extraction of (a) lower and (b) upper panels in Case 2 and (c) extension part in Case 3.

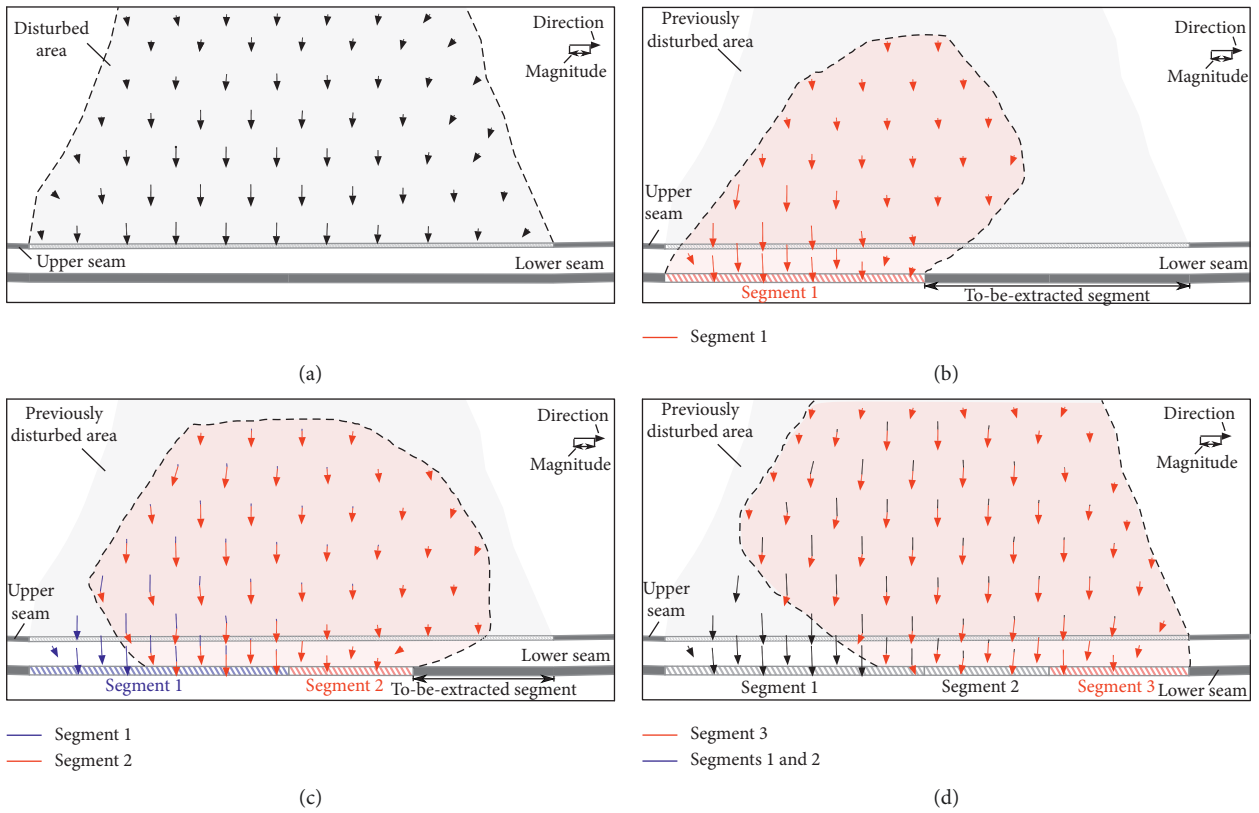

Figure 6: Deformation pattern after extraction of (a) lower panel and (b–d) different segments of the upper panel in Case 1.

ground movement above the previously extracted parts, especially above the edge of the extracted panel in Case 2 (Figure 8(a)). In addition, it can be seen that the angle of the major deformation pattern is significantly sharper after extraction of this segment in comparison with single-seam extraction. However, this angle becomes wider and similar to single-seam extraction by extracting the next segment of the extension part (Figure 8(b)).

4.2. Crack Propagation Pattern. The influence of the multiseam extraction on the crack propagation pattern can be studied by highlighting the areas of crack closure/opening after extraction of each segment of the multiseam panels. Different colors are used in Figures 9–11 to pursue this purpose. In order to separate the caved and fractured zones (Figure 1) the caved zone is chosen as the area with connecting interstrata fractures (vertical or semivertical fractures). The fractured area above the caved zone is then chosen as the fractured zone, which is located beneath the continuous deformation zone.

4.2.1. Case 1. After extracting the first segment of the lower panel, most of the existing cracks directly above the extracted segment are significantly altered (Figures 9(a) and 9(b)).

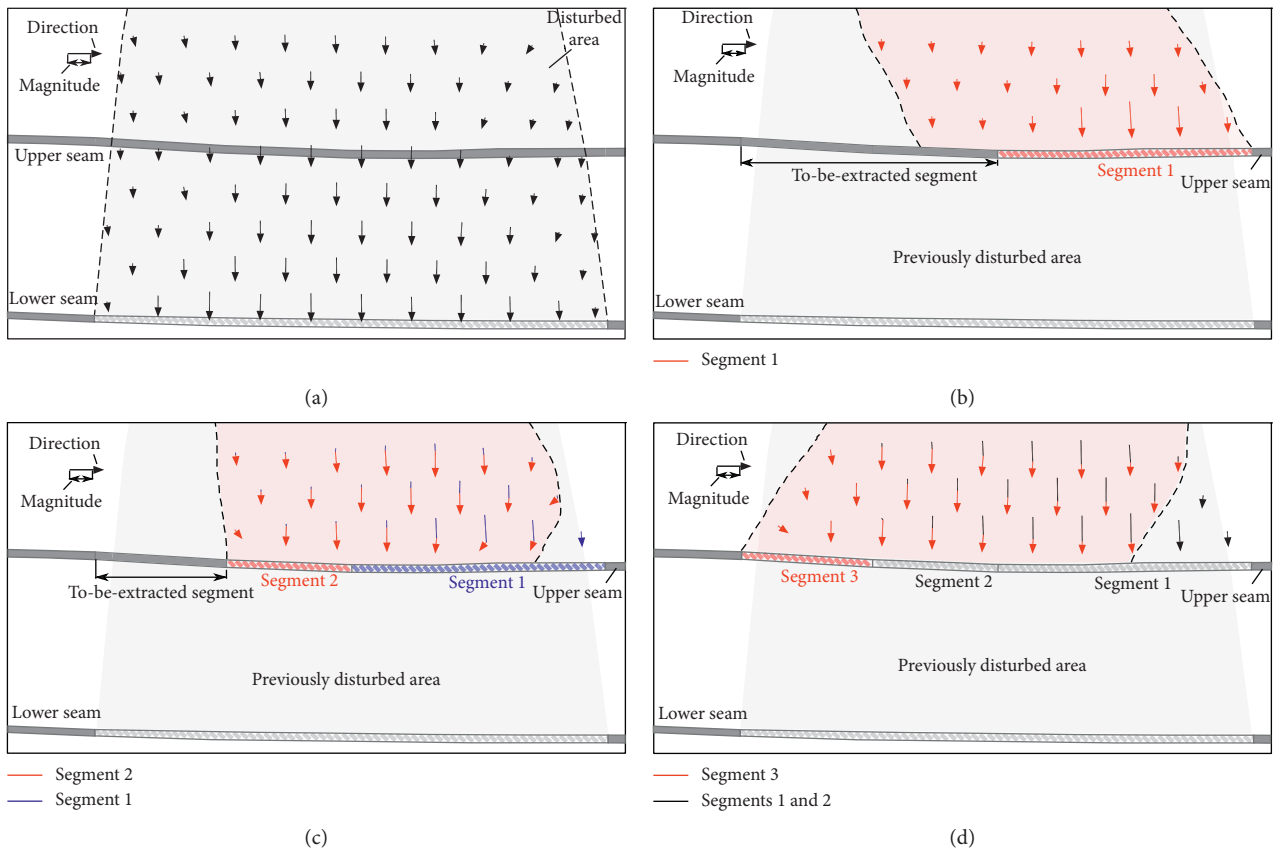

Figure 7: Deformation pattern after extraction of (a) lower panel and (b–d) different segments of the upper panel in Case 2.

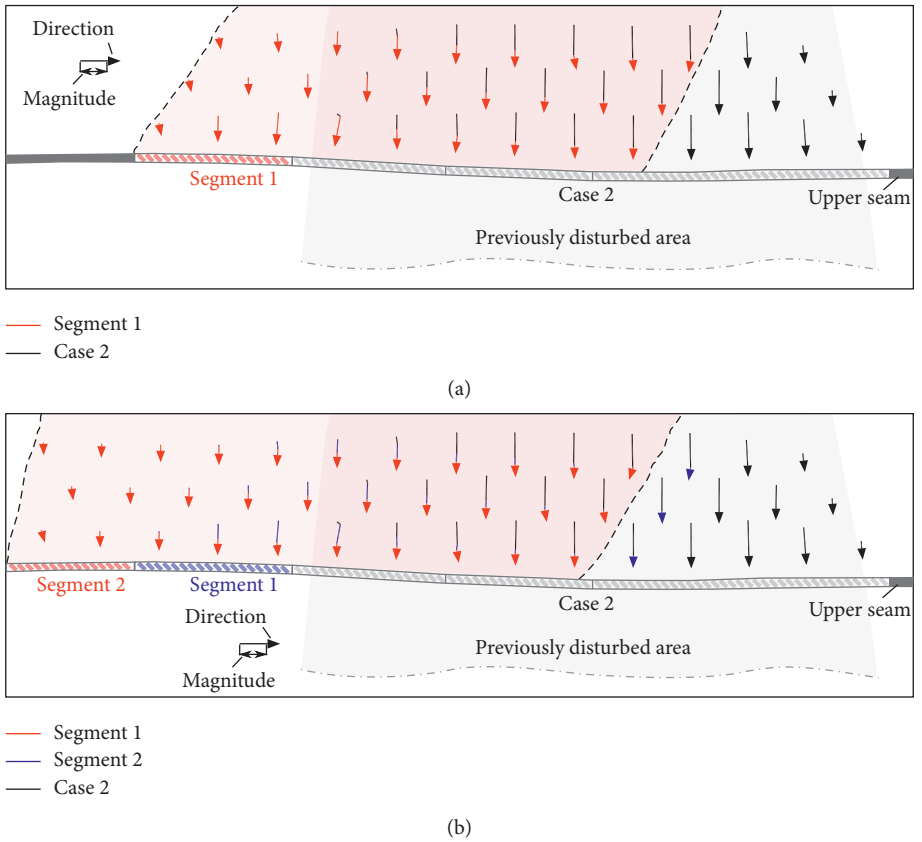

Figure 8: (a, b) Deformation pattern after extraction of different segments of the extension part in Case 3.

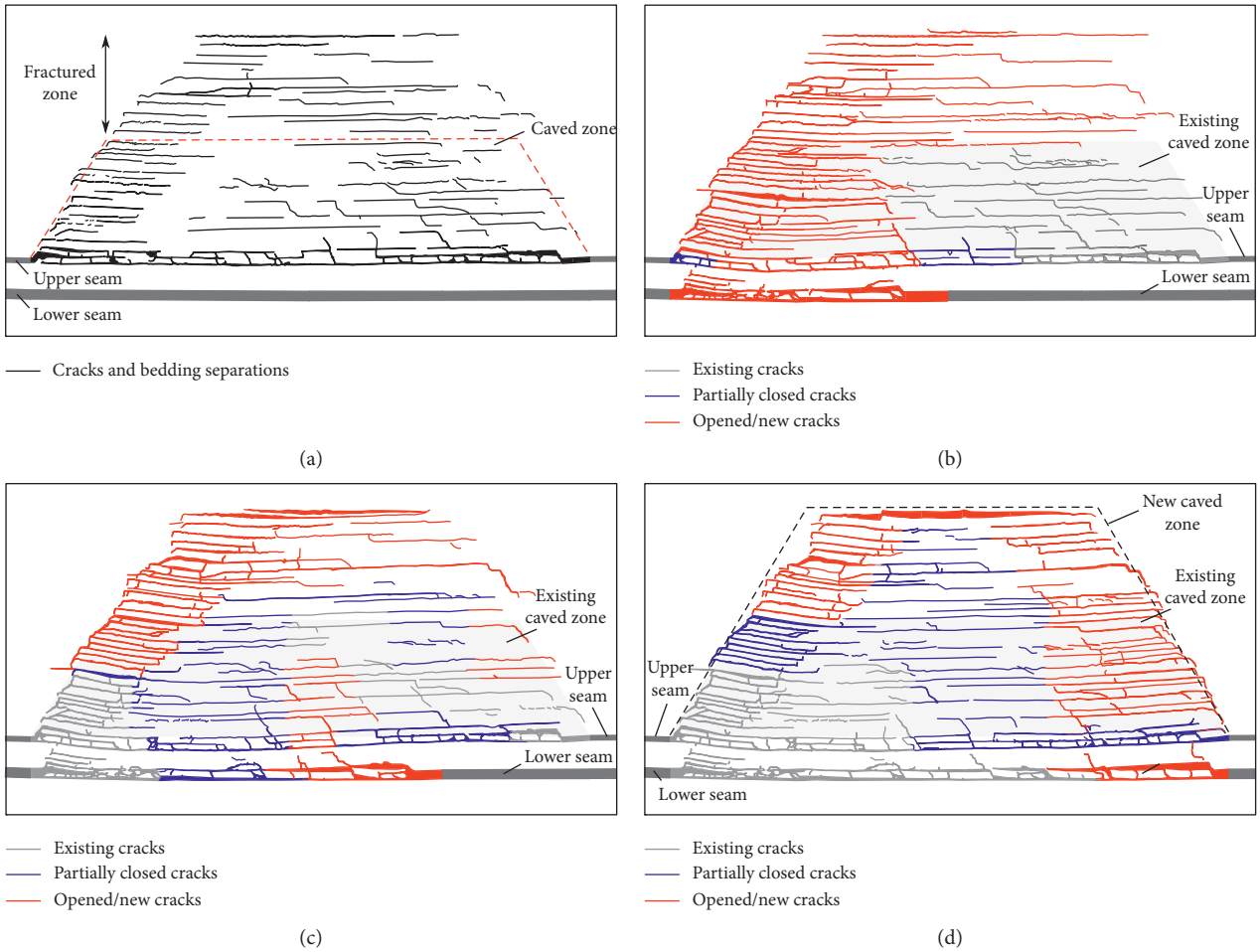

Figure 9: Crack propagation after extraction of (a) lower panel and (b–d) different segments of the upper panel in Case 1.

Extracting this segment also induces some crack opening above the to-be-extracted segments within the previously caved area. By advancing the lower panel extraction, major cracks above the previously extracted first segment partially closed or remained uninfluenced (blue and grey parts in Figure 9(c)). However, cracks and bedding separations in areas above this crack closure area predominantly opened (red parts in Figure 9(c)). Extraction of the third segment of the lower panel, similar to the second segment, induces partial closure of the cracks above the previously extracted segments (blue parts in Figure 9(d)) and creates new cracks and opens previously existing cracks and bedding separations above the newly extracted segment (red parts in Figure 9(d)).

One of the important observations from Figure 9 is that the caved zone after the lower extraction extends significantly towards shallower depths after extraction of the lower panel. The previously fractured area after the upper panel extraction becomes part of the caved zone of the multiseam extraction. In other words, extraction of the lower panel reactivates the fractured and previously disturbed areas and causes expansion of the connecting interstrata fractures. In addition, although extracting each new segment of the lower panel induces crack closure above the previously extracted segments, majority of cracks above the edges of the lower panel continue to open during the lower panel extraction.

4.2.2. Case 2. The fractured zone after extraction of the lower seam extends to the overburden layers above the upper panel (Figure 10). These fractures and bedding separations significantly influence the crack propagation pattern after extracting the first two segments of the upper panel. It can be seen that the previously formed bedding separations become mostly opened after extraction of the first and second segments (red parts in Figures 10(b) and 10(c)) and become mostly closed after completing the upper panel extraction.

By advancing the upper panel extraction (from segment 1 to 2, Figure 10(c), and from segment 2 to 3, Figure 10), cracks and bedding separations in areas above the previously extracted segments become partially closed (blue parts in Figures 10(c) and 10). Also, new cracks and bedding separations formed above the newly extracted segments. In addition, despite partial closure of most of the cracks above previously extracted segments, after extracting each new segment of the upper panel, previously existing cracks above the right edge of the upper panel (right edge of segment 1) continue to open during extraction of the whole upper panel.

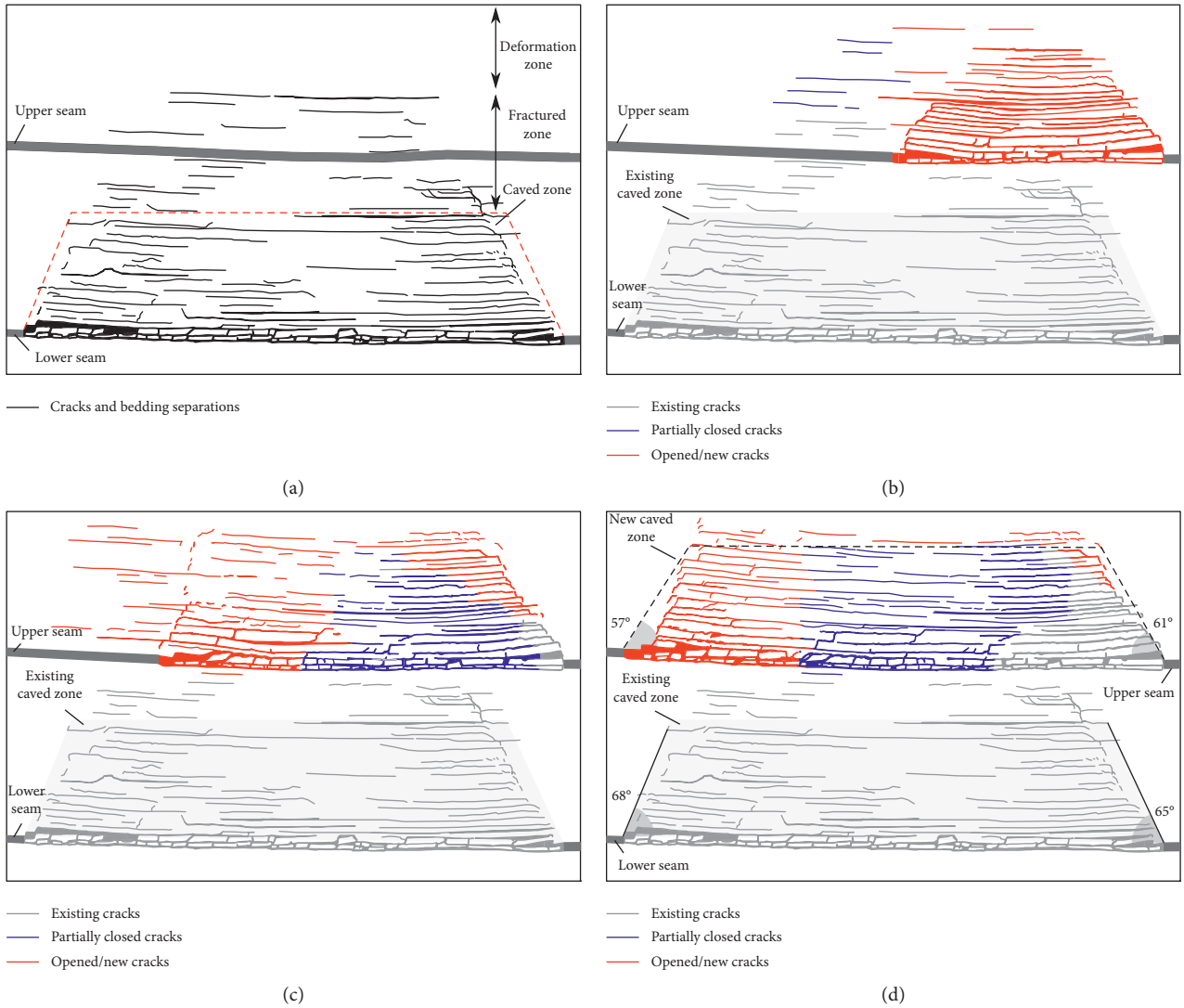

Figure 10: Crack propagation after extraction of (a) lower panel and (b–d) different segments of the upper panel in Case 2.

4.2.3. Case 3. Extraction of the extension part induces new fractures above the newly extracted segments and partially closes the previously existing cracks above the adjacent panel (Figure 11). Most of the interstrata fractures above the left edge of the upper panel in Case 2 become partially closed after extraction of the extension part (Figure 11(b)). In addition, the caved zone above the extended part is significantly smaller than the caved zone above the adjacent extracted panel (by comparison of Figures 11(b) and 10).

4.3. Angle of Break. Angle of break (or angle of major cracking) is defined as the angle that the limit of the major cracked area makes with horizon at the edge of an extracted panel. The angle of break indicates the limit of the severely disturbed zone above the edges of longwall panels.

Comparing the angles of break after lower and upper panel extractions in Case 2 indicates that extracting upper layer in this case (multiseam extraction) creates a slightly smaller angle of break than the lower layer (single-seam extraction, by comparison of Figures 10(a) and 10). In addition, extracting the first segment of the extension part in Case 3 creates a noticeably sharper angle of break (Figure 11(a)) than that of the upper panel in Case 2 (Figure 10). This angle of break, however, after extracting the next segment of the extension part becomes larger and similar to the lower panel's angle of break (Figure 11(b)).

4.3.1. Subsidence Factor. To study the effect of multiseam mining on subsidence (vertical deformation of the strata), several survey lines were considered in the three case studies. Two survey lines at 40 m and 80 m above the upper and lower coal seams horizon in Case 1 and one survey line at 40 m above the upper and lower coal seams in Cases 2 and 3 were chosen (Figure 2). To reduce the effects of extraction thickness on magnitude of subsidence, a dimensionless factor is used as follows:

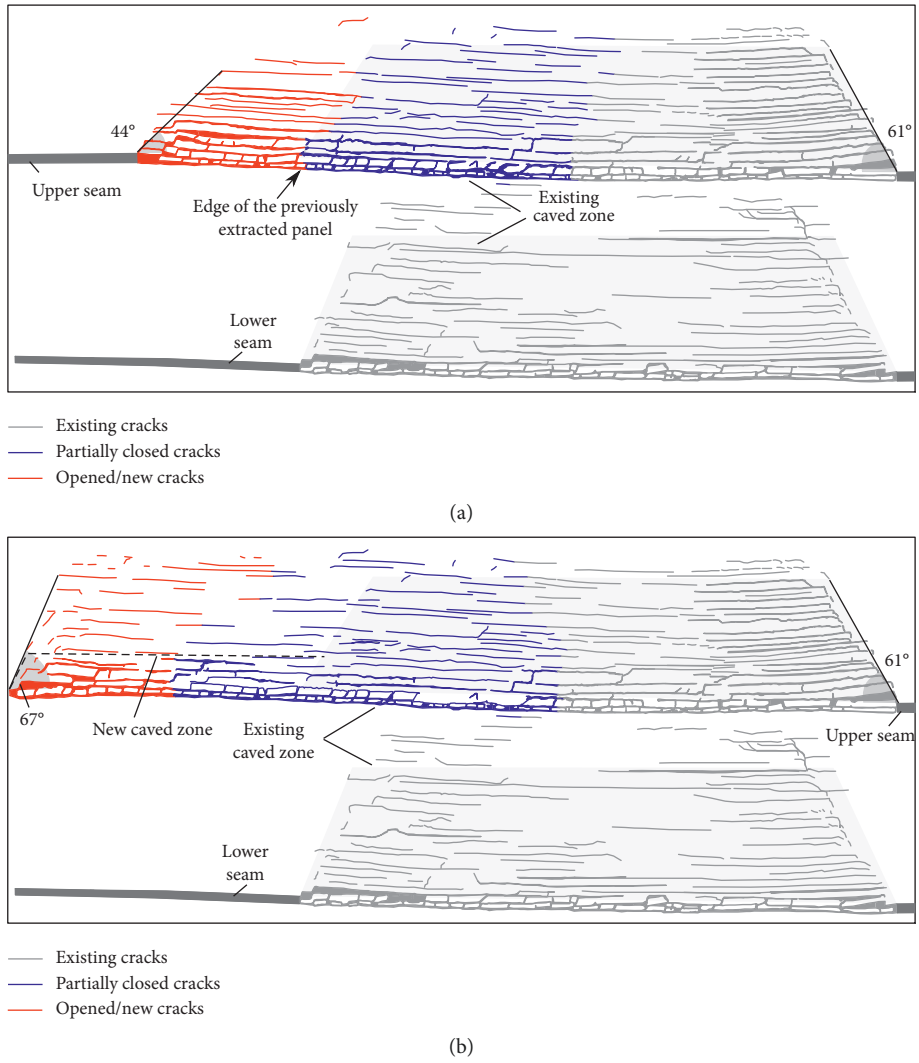

Figure 11: (a, b) Crack propagation after extraction of different segments of the extension part in Case 3.

$$\mathrm{SF} = \frac{S}{T}, \tag{3}$$

where SF is the subsidence factor at each survey point, S is the magnitude of subsidence at each survey point (m), and T is the average extraction thickness of the corresponding coal seam (m).

Investigating SF values for Case 1 shows that, at 40 m above the extracted panels, SF values after upper and lower panel extractions reach almost the same magnitude above the middle of the extracted panels (Figure 12(a)). However, at 80 m above the extracted panels, the lower panel creates much higher SF values in comparison with the upper panel. Also, the value of SF after the multiseam extraction at 40 m and 80 m in an area above the middle of the extracted panel is quite similar.

In Case 2, similar to Case 1, a significant increase in the value of SF is observed after extraction of the upper panel (Figure 12(b)). In this case, the magnitude of subsidence (S) at its maximum point exceeds the extraction thickness (T), resulting in a subsidence factor (SF) greater than one. In other words, strata subside more than the extracted thickness.

In both Cases 1 and 2, the maximum incremental subsidence ($\mathrm{SF}_{\max}$) after extraction of the multiseam panel occurs approximately above the middle of the extracted panel (Figure 12). However, $\mathrm{SF}_{\max}$ in Case 3 occurs above the previously extracted panel next to the extension part (Figure 12(b)).

5. Discussion

5.1. Strata Movement and Subsidence Analysis. The strata movement pattern for different cases shows that, after extraction of the multiseam panel, the strata tend to deform mainly within the borders of the previously disturbed area and only small deformations happen outside this area. This phenomenon was particularly evident in the undermining case with a thin interburden (Case 1; Figure 6(d)). In addition, the increase in the magnitude of subsidence factor after extracting the lower panel in Case 1 (Figure 12(a)) indicates that the disturbed strata subside significantly after extraction of the lower panel. These observations suggest

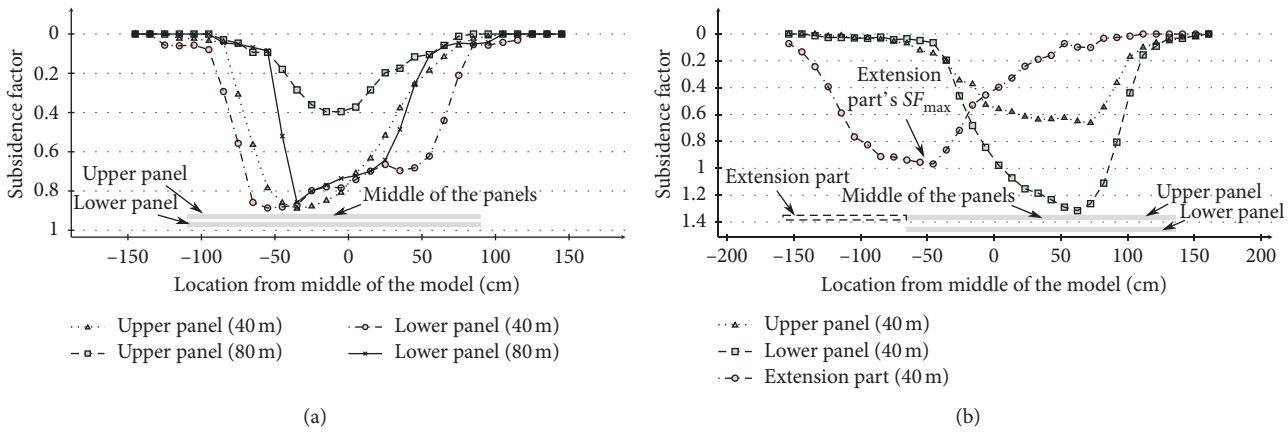

Figure 12: Magnitude of SF after extraction of each panel in (a) Case 1 and (b) Cases 2 and 3.

that the first mining activity reduces the bridging and load-carrying ability of the strata. As a result, after extracting the subsequent multiseam panels, the previously weakened strata deform and subside accordingly, creating an increased magnitude of subsidence. These previously weakened strata also provide the overburden layers with an alternative deformation path, which results in limiting the major deformations after the multiseam extraction to the previously weakened area.

In case of overmining a previously extracted panel (Case 2), interaction of the fractured and continuous deformation zones of the lower panel with the upper panel extraction alters the deformation pattern above the upper panel (Figure 7). After extraction of the upper panel in Case 2, previously existing fractures above the upper panel become partially closed (Figure 10). Closure of these fractures and the reduced bridging ability of the previously fractured strata create an increased magnitude of subsidence in the previously disturbed strata (Figure 12(b)).

In addition, existence of a previously extracted panel adjacent to the extension part in Case 3 alters the resultant deformation pattern after extracting the extension part in Case 3 (Figure 8). In this case, the newly undermined strata create a steep angle of major deformation. By moving further away from the previously caved zone, the resultant deformation pattern and the height of the caved zone above the extension part become similar to the single-seam observations (lower panel in Case 2; Figures 10(a) and 10). In addition, the maximum subsidence above the extension part in Case 3 occurs above the previously extracted adjacent panel and not above the newly extracted extension part (Figure 12(b)). Similar to the findings in [12], closure of the previously existing cracks above the edge of the adjacent panel is a reason for this observation.

5.2. Crack Propagation Pattern. Crack propagation pattern and the shape of the caved zone after extracting longwall panels are of great importance in determining the risk of water inrush and suitable location for the gas drainage boreholes [2, 6, 7, 17, 26]. The physical modelling results show that crack propagation pattern and shape of the caved zone after multiseam extractions are notably different from those after single-seam extractions.

Comparing the angle of break in different tests indicates variations in the crack propagation pattern depending on the arrangement of the panels. For instance, it can be seen that extracting the upper layer in Case 2 (multiseam extraction) creates smaller angle of break than the lower layer (single-seam extraction; Figures 10(a) and 10). This observation shows the effect of the previously caved zone that creates a weakened zone in the middle of the upper panel. The weakened zone changes the crack propagation pattern around the edges of the upper panel by inducing an alternative deformation path towards this area.

In addition, in Case 3, extending the upper panel creates a noticeably sharper angle of break than that in Case 2 (by comparison of Figures 10 and 11(a)). This observation also shows that presence of the previously caved area adjacent to the newly undermined section provides the newly undermined strata with an alternative deformation path, creating a sharp angle of break (Figure 11(a)). The angle of break, however, after extracting the next section of the extension part becomes larger and similar to the lower panel's angle of break (Figure 11(b)). In other words, by moving further away from the previously caved zone, strata conditions around the edge of the extracted panel similar to a single-seam extraction and a wider angle of break (Figure 11) and a major deformed area (Figure 8) are observed.

5.3. Risk of Water Inrush. Hydraulic conductivity in the strata above the mining horizon is an important factor in determining the water inrush risk. There is a clear correlation between the density of the voids after the mining activity and the hydraulic conductivity [6, 7]. The fracture propagation pattern after the multiseam mining, as observed from the physical modelling results, showed that the previously existing fractures close to the abutment area continue to open during the multiseam extraction. This increase in the density and connectivity of the fractures in this area is significantly greater than that in single-seam extraction. This was particularly observed in Cases 1 and 2 (Figures 9 and 10), while in Case 3, the crack propagation pattern above the

left edge of the extension part was similar to that in single-seam extraction (Figure 11(b)). In contrast, most of the fractures above the middle of the multiseam panels and close to the mining horizons become partially closed after undergoing an interim opening period during sequential extraction of multiseam panels (Figures 9 and 10). This observation is similar to reported field measurements for single-seam extractions in [27], where the hydraulic conductivity of the disturbed strata was measured to be significantly higher above the edges of the longwall panels in comparison with their center. However, the area, density, and connectivity of the fractures after multiseam extractions are significantly increased, as per observations from the physical modelling (Section 4.2).

Multiseam extraction also increases the fracture density, especially bedding separations and horizontal fractures above the middle of the extracted panels and close to the top of the caved area (Figure 13). Previously existing isolated horizontal fractures (bedding separations) within the fractured zone after extracting the first seam (Figure 13(a)) if interact with underground water can become filled with water over time (between single- and multiseam operations). Extracting multiseam panels would create a network of interstrata fractures that can reach the height of the previously existing fractured zone (Figure 13(b)). This connected fracture network can potentially provide the stored water in the horizontal fractures with a path towards the abutment area, from which the water can be led to the working spaces.

In addition, physical modelling results showed that the height of the caved zone after multiseam extraction in Case 1 has almost doubled (Figure 9). The increased hydraulic conductivity of the strata, as a result of the increase in the density of fractures and height of the caved zone after multiseam extraction, is of significant importance when undermining aquifers. This increase in the density and connectivity of the fractures poses a serious threat to the safety of machinery and personnel, which has to be controlled and mitigated. As a result, in multiseam extraction under aquifers, suitable risk management policies need to be taken. Some examples of these policies can be stated as follows:

(a) Use of backfill materials: this is particularly of interest in shallow mining under waterbeds or deep mining, where surface access to the mine area is limited.

(b) Grout injection from the surface or workings above the to-be-extracted longwall panels to increase the bridging ability of the strata and reduce bedding separations.

(c) Reducing the extraction width and/or increasing pillar widths in order to reduce the height of the caved zone.

(d) Changing the multiseam mining configuration and the arrangement of the panels, e.g., reducing the overlapping width of the panels by arranging longwall panels in staggered positions in the two mining seams (edge of the lower panel under the middle of the upper panel). In this regard, it was observed in Section 4.2.3 that the crack propagation pattern in Case 3 became similar to that in single-seam extraction by moving further away from the overlapping area of the previously extracted panels, i.e., smaller caved zone and less density and connectivity of induced fractures than multiseam extraction.

Importance of the multiseam mining configuration on the resultant ground movements has been emphasised and discussed in the literature [19, 23]. In this regard, the length of overlapping and positioning of the edges of the longwall panels in the two mining seams play a significant role in the crack propagation pattern and the resultant subsidence profile. The smaller the length of overlapping is, the less significant the multiseam interactions would be. Readers can refer to the published works in [19, 23] for more information about importance of the multiseam configuration on the associated fracture propagation and ground movements.

5.4. Gas Drainage Planning. One of the key factors in determining suitable locations for drilling gas drainage boreholes is the fracture propagation pattern after longwall extraction [2, 26]. Longwall mining-induced caved and fractured zones change the permeability in the overlying strata, releasing the gas in the coalbeds and more significantly in other porous formations in the overburden layers [4, 8]. Induced fractures in the caved and fractured zones increase the hydraulic conductivity and permeability of the disturbed strata. In this regard, identification of areas with high interstrata (vertical fractures) and horizontal (bedding separations) permeability is of great importance. For instance, fractured areas above solid abutments provide a suitable flow path for coalbed methane gas. A case study is reported in [4, 8], in which the methane gas production was improved by 77% as a result of placing gas drainage boreholes at the end of the longwall panels in comparison with borehole locations at the centre line of the longwall panels. The end of a longwall panel is confined by three sides, which results in occurrence of a highly tensile fractured area close to the margin of the panel. These fractures along the perimeter of a longwall panel, as mentioned in [26], provide a "sweet spot" for gas drainage. On a section of a mine, abutment areas close to the edges of the panels possess this characteristic.

In both undermining and overmining cases (Cases 1 and 2), interstrata fractures above the multiseam panel edges grow throughout the extraction of the panel. It can be seen that density of these fractures in the abutment areas is significantly higher than that in single-seam extraction in both Cases 1 and 2 (by comparison of Figures 9(a) and 9(d) for Case 1 and Figures 10(a) and 10 for Case 2). In Case 3, vertical fractures occur with a high density and sharp angle of break after mining the first segment of the extension part. The fracture propagation pattern, however, after extracting the second segment of this extension part becomes similar to that in single-seam extraction (Figure 11). Similar to the vertical fractures, occurrence of horizontal bedding separations increases after multiseam mining activity. This increase is particularly apparent above the edges of the multiseam panels in Cases 1 and 2 (Figures 9(d) and 10). In

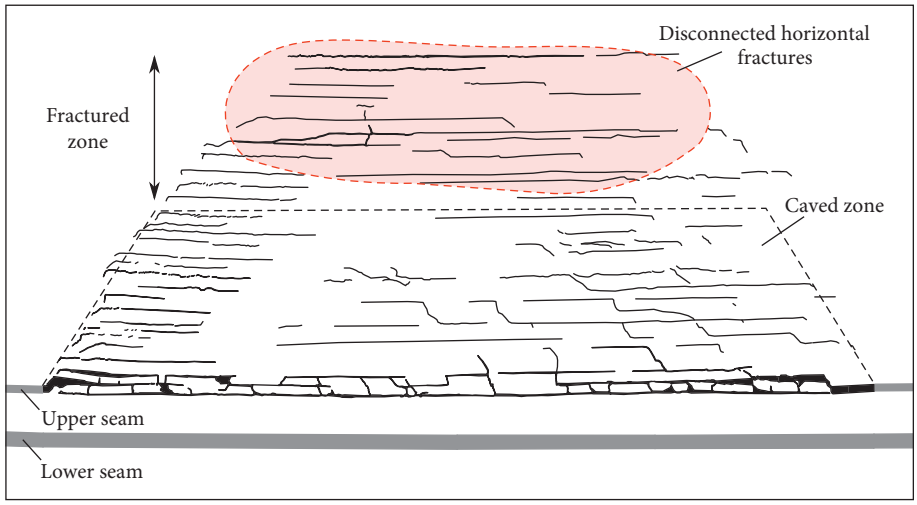

(a)

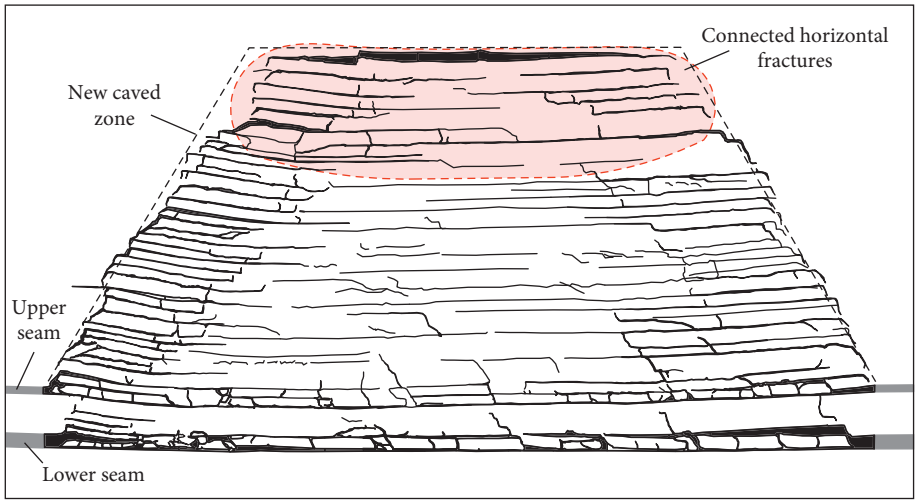

(b)

Figure 13: Changes in density and connectivity of horizontal fractures close to the top of the caved area after (a) single-seam and (b) multiseam extractions in Case 1.

addition, in Case 1, a significant increase in the number and size of bedding separations is observed above the middle of the multiseam panels and top of the newly caved area (Figure 9). In Case 2, similar to Case 1, bedding separations tend to occur mostly above the middle of the extracted panels (Figure 10). However, the increase in the density of bedding separations in Cases 2 and 3 is smaller than that in Case 1, which is likely to be related to the increased thickness of the interburden.

Based on the physical modelling results, potential suitable locations for placing the gas drainage boreholes after multiseam mining can be identified as the red-shaded areas in Figure 14. High density of horizontal and interstrata fractures above abutment areas, which continue to open throughout extraction of multiseam panels, creates a highly permeable zone for gas drainage. However, as mentioned in [26], methane gas flow is a dynamic process, which is influenced by strata destressing and fracture growth after longwall mining. As a result, dynamic methane gas flow and change of strata permeability during extraction of a longwall panel also need to be considered in determination of suitable gas drainage borehole locations.

6. Conclusions

Multiseam longwall mining-induced strata deformation and fracture propagation pattern can be studied by scaled physical modelling techniques. As demonstrated in the physical models, the strata deformation and fracture propagation patterns are different between multiseam and single-seam extraction cases. Red shadings show high-density interstrata and horizontal fractured areas, blue

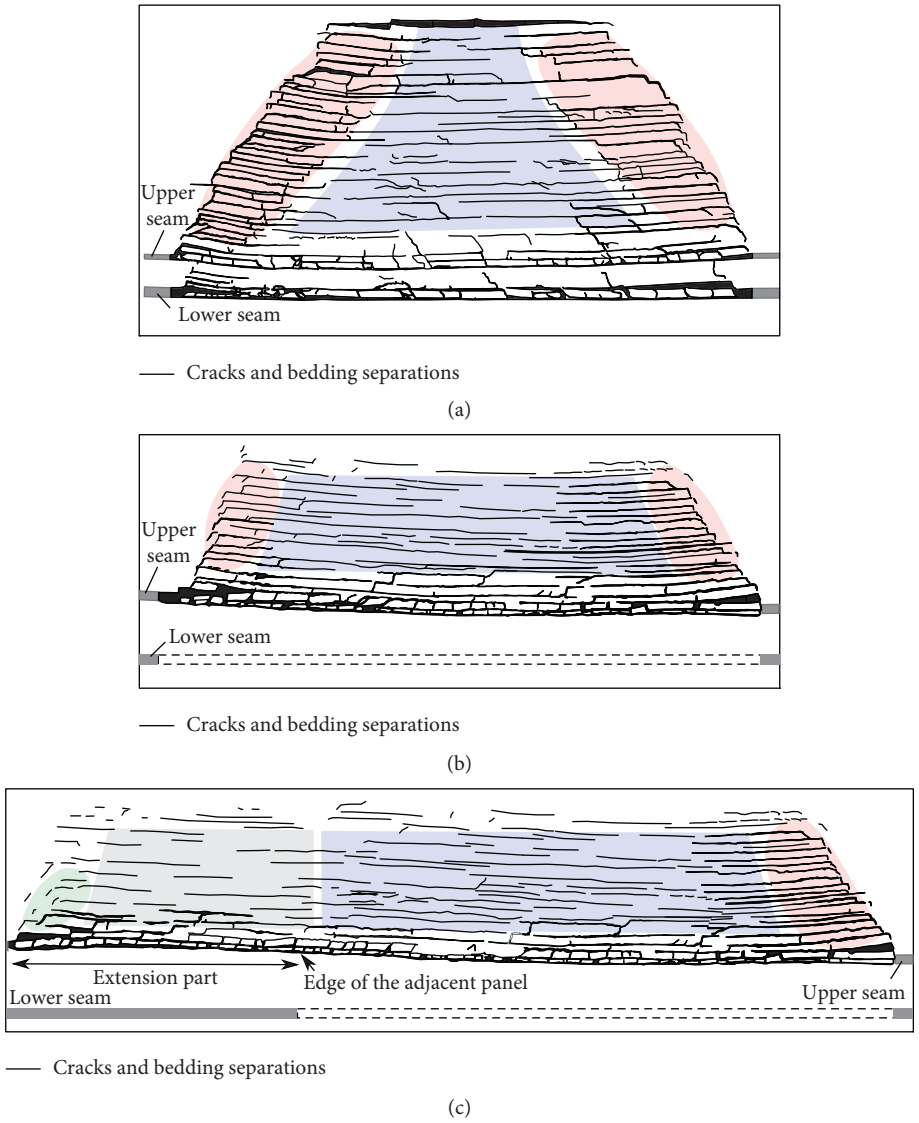

Figure 14: Interstrata and horizontal fractures after multiseam extraction in (a) Case 1, (b) Case 2, and (c) Case 3.

shading shows high-density horizontal fractured areas, and grey and green shadings show low-density horizontal and interstrata fractured areas, respectively.

These differences result in variations in the resultant multiseam subsidence profiles. Also, the induced caved and fractured zones influence the hydraulic conductivity of the strata, which is of great importance in evaluation of water inrush risk and determination of suitable productive locations for placing methane gas drainage boreholes.

Physical modelling techniques were used in this study to investigate differences between strata movement characteristics and fracture propagation pattern after single- and multiseam extractions. Three different case studies were modelled with varying mining configurations and interburden thicknesses. By monitoring the strata deformation and fracture propagation patterns after sequential extraction of multiseam panels by photogrammetry methods, variations in the resultant subsidence profiles and hydraulic conductivity of the caved and fractured strata were studied.

General conclusions drawn from the physical modelling results presented in this study can be summarised as follows:

(a) Multiseam mining in both cases of undermining and overmining of a previously extracted panel results in an enhanced magnitude of subsidence in comparison with single-seam mining. This is due to the reduced bridging ability of the caved and fractured strata, and also closure of previously opened fractures in the caved and fractured zones resulted from the previous mining activity. This phenomenon was observed in the case study with a thick interburden (Case 2 to a lesser extent in comparison with multiseam extraction with a thin interburden in Case 1).

(b) Existence of previously extracted multiseam panels adjacent to a newly extracted part significantly affects the mechanical response of the newly undermined strata. Major deformations occur close to the previously extracted area, and a sharp angle of break is

formed. Maximum subsidence also occurs close to the edge of the previously extracted adjacent panel, not above the newly extracted part. However, by moving further from the previously extracted areas, caving process and fracture propagation pattern become similar to those in single-seam mining.

(c) Previously existing fractures following single-seam extraction undergo dynamic changes after subsequent extraction of multiseam panels. These fractures predominantly tend to open at the area above/ahead of the newly extracted segment and partially close above the previously extracted segment of the multiseam longwall panel.

(d) Undermining of a previously extracted longwall panel results in significantly increased height of the caved zone. Interconnected fractures (both horizontal and interstrata) above the multiseam extraction provide a potential water flow path towards workings, which would pose a significant threat to safety of machinery and personnel in case of mining under aquifers. In this case, suitable measures need to be considered to mitigate and control the risk of water inrush, such as using backfill, grout injection into the overburden strata prior to multiseam extraction, reducing the width of the panel or increasing the width of chain pillars, and changing the arrangement of the multiseam panels (mining configuration).

(e) Density of fractures (both horizontal and interstrata) in all cases continues to increase during multiseam extractions over the edges of the multiseam panels, which results in increased hydraulic conductivity of the strata. As a result, abutment areas close to the edge of the longwall panels would be suitable locations for placing gas drainage boreholes.

(f) Interburden thickness affects the influence of the previously extracted panel on the strata movement characteristics by reducing the interaction of the caved and fractured zones of the two mining activities.

It can be seen that the scaled physical model is a useful technique in studying the strata movement patterns in relation to methane gas drainage planning and water inrush risk management. The complexity of multiseam interactions and the development of progressive fracture propagation patterns can be well illustrated via physical models. However, it should be mentioned that site-specific parameters and operational factors play a significant role in strata response to multiseam mining. Although physical modelling techniques provide invaluable insights into the mechanical behaviour of strata under specific conditions if complied with laws of similarity theory, care must be taken into consideration for employing these results in real cases.

Data Availability

Corresponding authors may provide the original data for discussion and communication for this study upon request.

Conflicts of Interest

The authors declare that they have no conflicts of interest.

Acknowledgments

This work has been conducted with support from the National Natural Science funded projects (award nos. 51504007 and 51574007) to Zhang. We acknowledge the Huainan Mining Group, Huaibei Mining Group, and Anhui University of Science and Technology for access to the mine, data, and physical resources necessary to complete this work. Also, this study was partially supported by the Higher Degree by Research Publications Grant from RMIT University to Ghabraie. We acknowledge RMIT University for this support.

References

[1] S.S. Peng and H.S. Chiang, *Longwall Mining*, John Wiley and Sons, Inc., New York, 1984.

[2] H. Guo, L. Yuan, B. Shen, Q. Qu, and J. Xue, "Mining-induced strata stress changes, fractures and gas flow dynamics in multi-seam longwall mining," *International Journal of Rock Mechanics and Mining Sciences*, vol. 54, pp. 129–139, 2012.

[3] L. Ying-ke, Z. Fu-bao, L. Lang, L. Chun, and H. Shen-yong, "An experimental and numerical investigation on the deformation of overlying coal seams above double-seam extraction for controlling coal mine methane emissions," *International Journal of Coal Geology*, vol. 87, no. 2, pp. 139–149, 2011.

[4] C. Ö. Karacan, F. A. Ruiz, M. Cotè, and S. Phipps, "Coal mine methane: a review of capture and utilization practices with benefits to mining safety and to greenhouse gas reduction," *International Journal of Coal Geology*, vol. 86, no. 23, pp. 121–156, 2011.

[5] A. Majdi, F. P. Hassani, and M. Y. Nasiri, "Prediction of the height of destressed zone above the mined panel roof in longwall coal mining," *International Journal of Coal Geology*, vol. 98, pp. 62–72, 2012.

[6] W. X. Wang, W. H. Sui, B. Faybishenko, and W. T. Stringfellow, "Permeability variations within mining-induced fractured rock mass and its influence on groundwater inrush," *Environmental Earth Sciences*, vol. 75, no. 4, p. 326, 2016.

[7] J. Zhang and B. Shen, "Coal mining under aquifers in China: a case study," *International Journal of Rock Mechanics and Mining Sciences*, vol. 41, no. 4, pp. 629–639, 2004.

[8] C. Ö. Karacan, G. S. Esterhuizen, S. J. Schatzel, and W. P. Diamond, "Reservoir simulation-based modeling for characterizing longwall methane emissions and gob gas venthole production," *International Journal of Coal Geology*, vol. 71, no. 23, pp. 225–245, 2007.

[9] B. Ghabraie and G. Ren, "Mechanism and prediction of ground surface subsidence due to multiple-seam longwall mining," in *Proceedings of 35th International Conference on Ground Controlin Mining (ICGCM)*, pp. 304–310, Morgantown, WV, USA, July 2016.

[10] B. Ghabraie, G. Ren, J. Barbato, and J. V. Smith, "A predictive methodology for multi-seam mining induced subsidence," *International Journal of Rock Mechanics and Mining Sciences*, vol. 93, pp. 280–294, 2017.

[11] B. Ghabraie, G. Ren, and J. V. Smith, "Characterising the multi-seam subsidence due to varying mining configuration,

insights from physical modelling," *International Journal of Rock Mechanics and Mining Sciences*, vol. 93, pp. 269–279, 2017.

[12] B. Ghabraie, G. Ren, X. Zhang, and J. Smith, "Physical modelling of subsidence from sequential extraction of partially overlapping longwall panels and study of substrata movement characteristics," *International Journal of Coal Geology*, vol. 140, pp. 71–83, 2015.

[13] A. M. Suchowerska, J. P. Carter, and R. S. Merifield, "Horizontal stress under supercritical longwall panels," *International Journal of Rock Mechanics and Mining Sciences*, vol. 70, pp. 240–251, 2014.

[14] G. Li, P. Steuart, and R. P^aquet, "A case study on multi-seam subsidence with specific reference to longwall mining under existing longwall goaf," in *Proceedings of the Seventh Triennial Conference on Mine Subsidence*, pp. 111–125, Sydney, NSW, Australia, November 2007.

[15] G. Ren, G. Li, and M. Kulessa, "Application of a generalised influence function method for subsidence prediction in multi-seam longwall extraction," *Geotechnical and Geological Engineering*, vol. 32, no. 4, pp. 1123–1131, 2014.

[16] P. R. Sheorey, J. P. Loui, K. B. Singh, and S. K. Singh, "Ground subsidence observations and a modified influence function method for complete subsidence prediction," *International Journal of Rock Mechanics and Mining Sciences*, vol. 37, no. 5, pp. 801–818, 2000.

[17] W. Sui, Y. Hang, L. Ma et al., "Interactions of overburden failure zones due to multiple-seam mining using longwall caving," *Bulletin of Engineering Geology and the Environment*, vol. 74, no. 3, pp. 1019–1035, 2014.

[18] T. Unlu, H. Akcin, and O. Yilmaz, "An integrated approach for the prediction of subsidence for coal mining basins," *Engineering Geology*, vol. 166, pp. 186–203, 2013.

[19] J. M. Galvin, *Ground Engineering—Principles and Practices for Underground Coal Mining*, Springer International Publishing, Berlin, Germany, 1st edition, 2016.

[20] B. Ghabraie, G. Ren, J. Smith, and L. Holden, "Application of 3D laser scanner, optical transducers and digital image processing techniques in physical modelling of mining-related strata movement," *International Journal of Rock Mechanics and Mining Sciences*, vol. 80, pp. 219–230, 2015.

[21] B. Ghabraie, K. Ghabraie, G. Ren, and J. V. Smith, "Numerical modelling of multistage caving processes: insights from multi-seam longwall mining-induced subsidence," *International Journal for Numerical and Analytical Methods in Geomechanics*, vol. 41, no. 7, pp. 959–975, 2016.

[22] G. Li, P. Steuart, R. P^aquet, and R. Ramage, "A case study on mine subsidence due to multi-seam longwall extraction," in *Proceedings of Second Australasian Ground Control in Mining Conference*, pp. 191–200, Sydney, NSW, Australia, November 2010.

[23] B. Ghabraie, *Multi-seam mining-induced ground surface subsidence, characteristics and prediction*, Ph.D. thesis, School of Engineering, RMIT University, Melbourne, Australia, 2016.

[24] B. N. Whittaker and D. J. Reddish, "Preface," in *Subsidence Occurrence, Prediction and Control, Developments in Geotechnical Engineering*, B. N. Whittaker and D. J. Reddish, Eds., vol. 56, pp. 5-6, Elsevier, Amsterdam, Netherlands, 1989.

[25] Z. Weishen, L. Yong, L. Shucai, W. Shugang, and Z. Qianbing, "Quasi-three-dimensional physical model tests on a cavern complex under high in-situ stresses," *International Journal of Rock Mechanics and Mining Sciences*, vol. 48, no. 2, pp. 199–209, 2011.

[26] H. Guo, C. Todhunter, Q. Qu, and Z. Qin, "Longwall horizontal gas drainage through goaf pressure control," *International Journal of Coal Geology*, vol. 150-151, pp. 276–286, 2015.

[27] Y. Li, "Groundwater system for the periods of pre- and post-longwall mining over thin overburden," *International Journal of Mining, Reclamation and Environment*, vol. 30, no. 4, pp. 295–311, 2015.